Complementary Use of Wearable Technology 4: Assessing Gait Asymmetry and Shock Attenuation Using Multiple IMU Devices

Jay H. Williams, [1] **Samuel F. Rizzuto,** [1] **Brandon A. Dillard ,** [2] **Emily J. Whitaker** [2]

[1]Department of Human Nutrition, Foods and Exercise, Virginia Tech, Blacksburg, VA 24061 USA
[2]Department of Athletics, Virginia Tech, Blacksburg, VA 20401 USA

Wearable technology | Accelerometry | Shock attenuation | Gait symmetry | ACL injury

Headline

In the previous study (16) we developed procedure to temporally synchronize and align data from multiple IMUs. The results showed that accelerometer signals from the IMeasureU Blue Trident sensor (BT-IMU) and STATSports APEX unit can be synchronized and, once synchronized, show considerable similarity. This raises the possibility of coupling raw accelerometer data generated from the APEX sensor (e.g. speed, trunk acceleration and angular velocity) with data from the BT-IMU (ankle acceleration and angular velocity).

Aim

The aim of this study was to determine the feasibility of deriving spatiotemporal and shock attenuation characteristics by merging acceleration, angular velocity and speed data from distinct GPS-IMU devices. Proof of concept was established by analyzing data derived from the APEX and BT-IMU devices across a range of running activities as well as comparing data from healthy and injured individuals.

Methods

Technology

As previously described (16), two types of IMU sensors were used. The STATSports APEX GPS/IMU (18 Hz GPS, ±200g 952 Hz tri-axial accelerometer, 952 Hz gyroscope and 10 Hz magnetometer) and the IMeasureU Blue Trident (BT-IMU) IMU (±16 g 1125 Hz and ±200 g, 1600 Hz accelerometers, 1125 Hz gyroscope and 112 Hz magnetometer). Prior to training, all devices were turned on 30 min prior to use. Following each session, data from the APEX and BT-IMU devices were downloaded using the SONRA and IMU Step software and into individual drills or events. Raw data were then exported to individual .csv files for further analysis. All subsequent analyses were performed using custom written MATLAB programs.

A single APEX unit was placed inside of a pouch located on the back of a manufacturer-supplied vest (similar to a sports bra). This situated the trunk-mounted device near the upper cervical vertebrae. Two BT-IMU sensors were attached to the lower leg using silicone straps provided by IMeasureU. This placed the ankle-mounted devices slightly above the medial malleolus. Care was taken to ensure a snug fit of all three devices to minimize unwanted movements.

Subjects

Participants for this study were six collegiate female soccer players (age 19.1 ± 1.0 years, height 158.3 ± 4.0 cm, weight 55.2 ± 2.3 kg, $\bar{x}$ ±SD). Three of the players had suffered prior anterior cruciate ligament tears and were undergoing rehabilitation (approximately 20 weeks post-surgery). The remaining three had no history of knee, hip of ankle injury. Institutional review and human subjects use approval was acquired and subject consent obtained prior to data collection. Subjects were asked to perform several running trials 100-200m in length at varying speeds.

Data Collection and Analysis

Calibration Routine. As in the previous paper (16), temporal alignment of accelerometer signals can be accomplished by applying controlled impacts to all sensors simultaneously. Prior to and immediately after each session, three impacts were applied as described previously. Those data were then subjected to cross-correlation analysis to determine the time delay (TD) between the BT-IMU and APEX sensors. The derived TD was then used to synchronize data from the remainder of the session. TD between the devices, obtained before and after training did not differ.

Temporal Alignment. For each session, accelerometer, gyroscope and velocity data from the three devices were re-sampled to 1000 Hz. They were then low-pass filtered at 40 Hz using a fourth-order Butterworth filter. The TD determined above was then applied to the BT-IMU and APEX data to temporally align the accelerometer and gyroscope data. Figure 1 shows a segment of accelerometer data from the three devices prior to and after the alignment procedure. In this example, the BT-IMU signals were found to lag behind the APEX device by 142 msec. After application of this TD, they are more closely aligned.

Spatiotemporal Variable Determination. Foot strike (FS) and toe off (TO) were determined for each limb as described previously (1, 7, 9) using the BT-IMU gyroscope data adjusted using the TD (see Figure 2). From the pitch gyroscope data, peak angular velocity of the swing phase was determined (midswing, MS). Using MS as a starting point, the data were searched backwards and forwards for the local minima on either side of MS. The local minimum prior to MS was identified as the TO of the previous stance phase and the local minimum after MS was identified as the FS of the subsequent stance phase. The interval between consecutive FS and TO values was defined as contact time (CT). Temporal variables were derived using the FS and TO data from the right and left limbs. A step was defined as the interval from bilateral

FS values (right-to-left and left-to-right). The spatial variable step length was derived by multiplying average running speed during the step (obtained from the APEX GPS data) times by the step time.

For each of the spatiotemporal variables, symmetry was defined as the bilateral difference between limbs using the equation below. For the control players x_1 and x_2 represented left and right limb values, respectively. For the ACL players, the two parameters represented values from the healthy and injured limbs, respectively. Using this equation, a value of zero represents perfect symmetry between limbs. Larger positive or negative values indicate increasing asymmetry.

$$Symmetry(\%) = 200 \times [(x_1 - x_2)/(x_1 + x_2)]$$

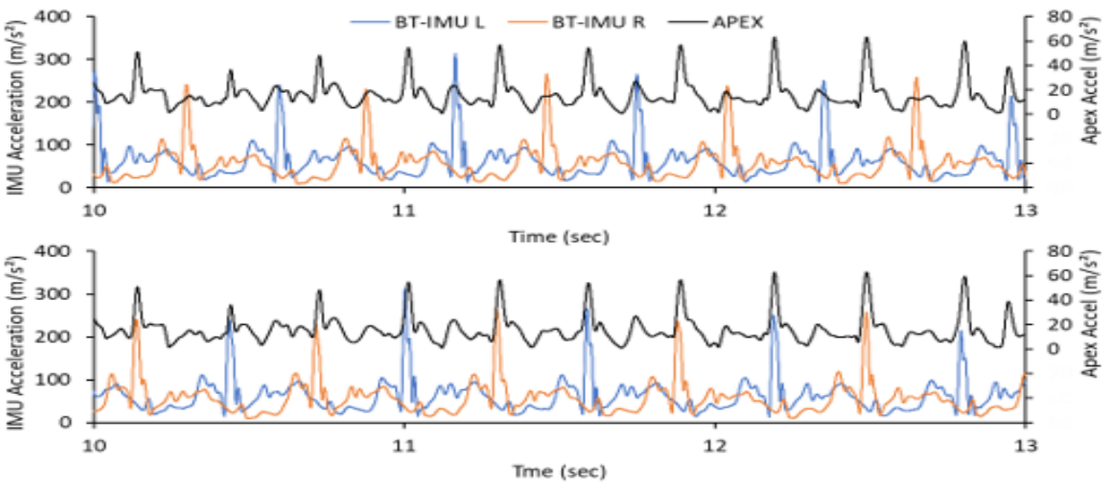

Fig. 1. Raw APEX and BT-IMU accelerometer signals recorded during running. Top: Signals before time delay adjustment. Bottom: The same signals after shifting the BT-IMU signals forward by the calculated TD.

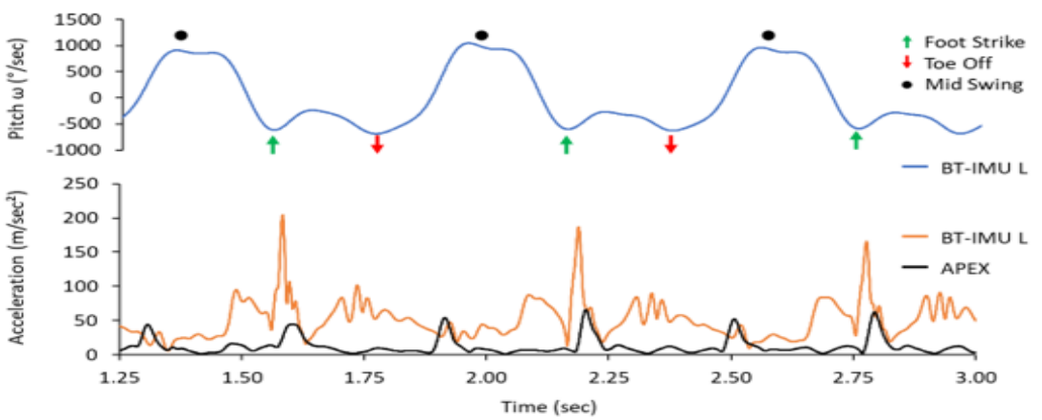

Fig. 2. Top: Detection of initial foot strike (FS) and subsequent toe off (TO) using pitch angular velocity measures of the left ankle. Bottom: Accelerations at the ankle (BT-IMU) and trunk (APEX). Trunk acceleration peaks situated between ankle peaks represent right foot ground contacts.

Shock Attenuation. During each stance phase (or CT interval), accelerations recorded at the trunk are attenuated compared to those recorded at the ankle. For this study, peak attenuation was computed for each limb using peak trunk and ankle resultant accelerations (aAPEX and aBT-IMU) during the stance phase using the equation below (4, 14). Increasing peak attenuation indicates increased dampening of the acceleration signal from the ankle to the trunk.

$$Peak\ Attenuation(\%) = 100 \times [1 - (a_{APEX}/a_{BT-IMU})]$$

Accelerations during the stance phase were also transformed into the frequency domain using Fast Fourier Transform. Shock attenuation was computed by first calculating the mean power spectral densities (PSD) of accelerations experienced during the stance phase of each limb using the BT-IMU and AEPX data. The following transfer function was then used to calculate shock attenuation (3, 15, 10). Values that are more negative indicate increased attenuation of the impact signal from the ankle to the trunk. For this study, mean PSD between 10 and 20 Hz, were compared, which represents the

portion of the PSD associated with foot strike (10, 11, 15).

$$Shock\ Attenuation(dB) = 10 \times \log_{10}(PSD_{APEX}/PSD_{BT-IMU})$$

Results

Running speed step time and step length during a single effort are shown in Figure 3. In this example, a non-injured player performed a 200m run in which running speed varied from a jog to a stride (∼5-20 km/hr). These data were chosen to exemplify changes the spatiotemporal variables as a function of speed. As can be seen, step time decreases with increases in running speed. Conversely, step length increases as the subject increases her running speed.

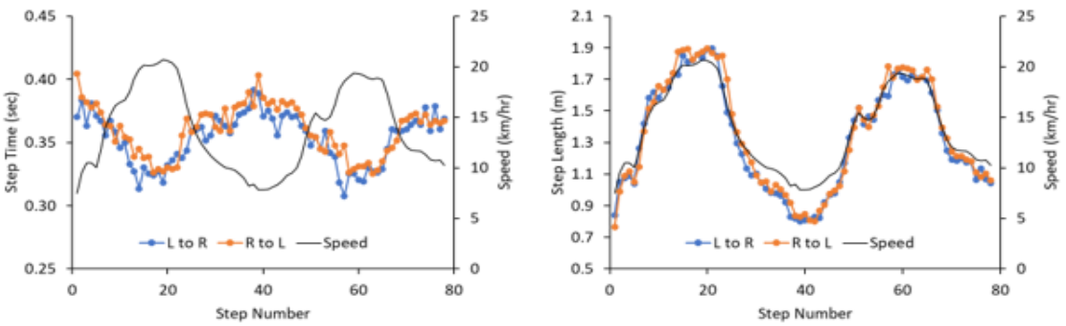

Fig. 3. Right and left step times and lengths during a 200m run with varying pace. Also shown is the running speed. Data are from a healthy subject. Each point represents a distinct step. Also shown in running speed.

Table 1. Spatiotemporal and symmetry data from Control and ACL injured players.

Variable	Control		ACL Injured	
	Left Left → Right	Right Right → Left	Healthy Healthy → Injured	Injured Healthy → Injured
CT (msec)	205.3 ± 10.1	202.6 ± 9.6	209.7 ± 11.2	201.6 ± 12.6
Symm (%)	2.66 ± 0.80		4.02 ± 1.95	
Step Time (msec)	312.6 ± 14.2	320.4 ± 13.6	322.3 ± 15.0	290.2 ± 16.2
Symm (%)	-2.48 ± 0.65		11.10 ± 3.02	
Step Length (m)	1.56 ± 0.52	1.62 ± 0.46	1.61 ± 0.53	1.42 ± 0.50
Symm (%)	-2.46 ± 0.54		13.38 ± 2.32	

Values are means ± SD

A comparison of mean spatiotemporal values for the healthy and injured players are shown in Table 1. These values were derived from players performing three, 100m runs at consistent pace of approximately 18km/hr. To ensure a constant pace, they were asked to complete the 100m in 20 sec while intermediate times were given. For the most part, right and left limb values for the control athletes are similar, with symmetry values $< 3\%$. However, the ACL injured players show differences between the healthy and injured limbs. In general, the non-injured limb values are similar to the non-injured players while the injured limb values tend to be reduced. This results in gait asymmetry of 4 and 13% with greater values associated with the healthy limb. For example, step length is about 13% longer in the healthy-to-injured step compared to the contralateral. Because of the small sample size, statistical comparisons were not made. As such, group differences shown here must be viewed carefully. Nevertheless, they do support the notion that the athletes undergoing ACL rehabilitation alter their gait, compensating for the surgical reconstruction.

Figures 4 and 5 show raw data used in the calculation attenuation variables. These data are from a healthy athlete performing a 100m run at approximately 14 km/hr. Shown are accelerations from the ankle and trunk during the stance phase (Figure 4). They emphasize the dampening or attenuation of the acceleration signal at the trunk. The peaks of these signals were used to calculate peak attenuation (right panel).

The frequency spectra of the ankle and trunk accelerations are shown in Figure 5. The portion of the spectra associated with foot strike is indicated by the red box. The right panel shows the shock attenuation across the frequency spectra calculated from the transfer function described earlier. In this example, left and right shock attenuations between 10 and 20 Hz were -6.31 and -6.19 dB.

As with the spatiotemporal variables, synchronizing the APEX and IMU data allows attenuation to be calculated for

each step. This is shown in Figure 6 for a healthy athlete. Mean values for healthy and injured players, across the duration of the effort are shown in Table 2. As in Table 1, these data were collected during constant speed running at 18 km/hr. In the control subjects, both peak and shock attenuations were similar between limbs. This is not the case in the ACL athletes who show slightly reduced attenuation in the injured limb. Both peak and shock attenuation in the injured group appears to result from decreased peak acceleration and reduced PSD at the ankle of the injured limb (Table 2). However, due to limited subjects, group interpretations of the data remain speculative.

Figure 7 emphasizes the importance of tightly regulating or monitoring running speed during field testing. In this figure, athletes were asked to run 100m at three speeds: a jog, moderate-speed stride and high-speed stride. As in our previous study (17), there was some overlap in the actual speeds (determined via GPS). In addition, the data show increasing attenuation as speed increases. Thus, it is important when evaluating attenuation during running activities, speed be tightly controlled or monitored.

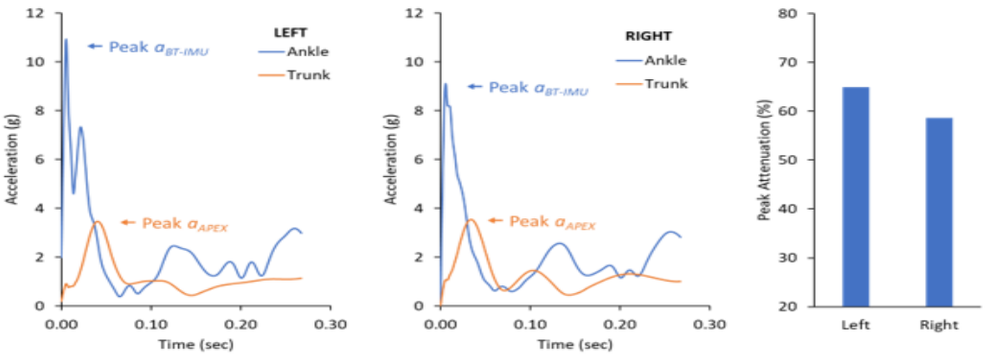

Fig. 4. **Peak accelerations for left and right steps and peak attenuation. Data are from a 100m bout performed at ~14 km/hr.**

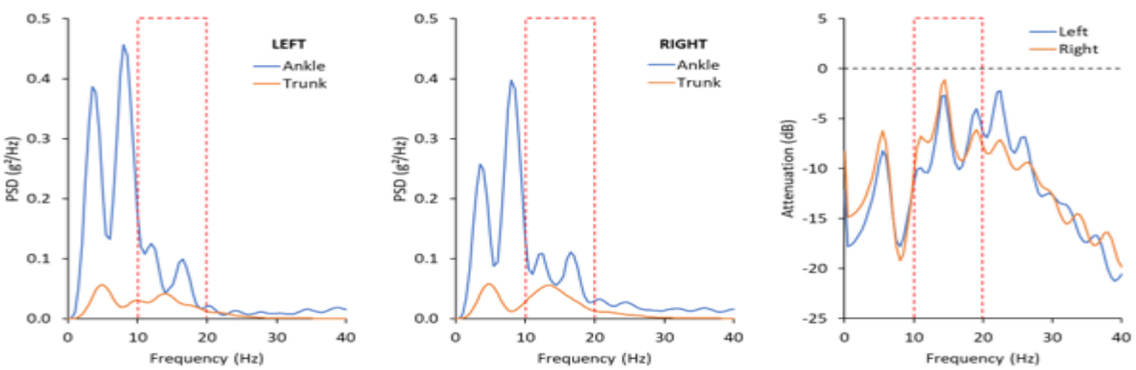

Fig. 5. **Power spectral densities and attenuation obtained from running at ~14 km/hr. Data are from a healthy athlete. The red boxes indicate the portion of the PSD associated with foot impact.**

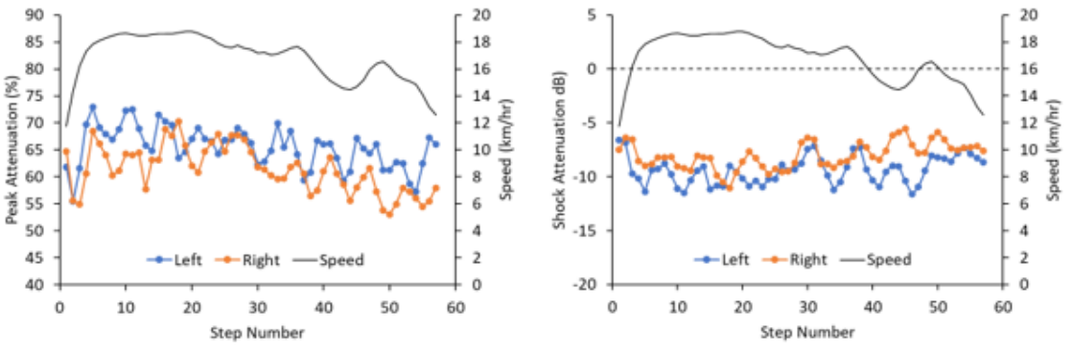

Fig. 6. **Peak (left) and shock (right) attenuation in right and left limbs during running at ~18 km/hr in a healthy subject.**

Table 2. Attenuation values from Control and Injured athletes.

	Control		ACL Injured	
Variable	Left	Right	Healthy	Injured
Peak Accel Ankle (g)	9.404 ± 2.445	9.365 ± 3.231	8.635 ± 2.986	6.352 ± 2.650
Peak Accel Trunk (g)	2.988 ± 1.016	3.057 ± 1.123	2.997 ± 1.032	2.737 ± 1.132
Peak Attenuation (%)	68.23 ± 4.60	67.36 ± 5.11	65.29 ± 4.77	56.91 ± 8.24
PSD Ankle (g^2/Hz)	0.0734 ± 0.0278	0.0724 ±0.0279	0.0672 ± 0.0255	0.0501 ± 0.0204
PSD Trunk (g^2/Hz)	0.0184 ±0.0068	0.0174 ± 0.0062	0.0165 ±0.0060	0.0188 ± 0.0073
Shock Attenuation (dB)	-6.10 ± 2.33	-6.19 ± 1.82	-5.95 ± 1.50	-4.26 ± 8.24

Values are means ± SD

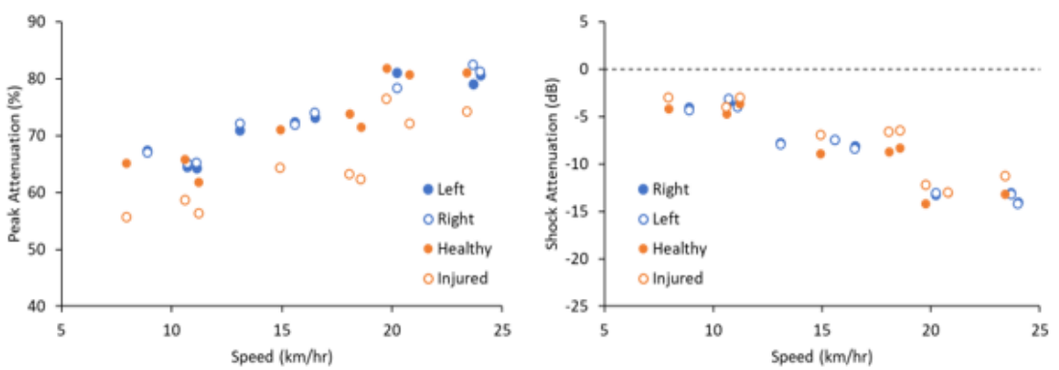

Fig. 7. **Changes in peak (left) and shock(right) attenuation with changes in running speed. Data were collected during three trials of approximately 10, 15 and 20 km/kr. Each symbol represents one step. Inset: running speed during the bout.**

Discussion

The results of this study show that data from ankle-mounted BT-IMU sensors and a trunk-mounted APEX device can be temporally synchronized. Also, the synchronized data can be used to compute spatiotemporal gait variables as well as attenuation of accelerometer signals. As these devices are routinely used by sports scientists to monitor load in competitive athletes, combining their data allows for more detailed examination of gait and gait symmetry. This can be particularly useful when monitoring rehabilitation of injured athletes.

We aimed to develop a method for combining data from the APEX and BT-IMU devices to generate metrics characterizing gait symmetry. Over the course of the study, a few pre-

liminary findings regarding potential differences in spatiotemporal and attenuation variables between healthy and injured athletes emerged. First, ACL injured athletes appear to have considerable spatiotemporal asymmetry during running. In the injured subjects, contact times appears to be less for the injured limb. Also, the step length and time is less when stepping from the healthy to the injured limb as opposed to the injured-to-healthy step. Second, both peak and shock attenuations seem to be decreased in the injured limb. This appears to results from reduced peak accelerations and PSDs at the ankle of the injured limb but not at the trunk. Others (2, 5, 6, 12) also show altered spatiotemporal characteristics following ACL reconstruction surgery.

Unfortunately, there appears to be little information on impact attenuation during running in ACL injured subjects. However, attenuation has be shown to be reduced following fatiguing activity in healthy individuals (3, 10). Some groups also suggest reduced quadriceps strength following ACL reconstruction could reduce the injured limb's ability to attenuate shock during running and landing activities (8, 13). Clearly, questions surrounding possible spatiotemporal and impact attenuation asymmetry in ACL injured individuals deserve future attention.

Figure 3 shows changes in step time and length with changes in running speed. Also, peak and shock attenuations increase as speed increases (Figure 7). Similar findings been reported by others (10, 11, 15). We show impact load and step balance are also dependent on speed (17). Taken together, these findings emphasize the importance of combining GPS-derived speed data with accelerometer and gyroscope data when analyzing gait. It can be difficult to control running speed when gait evaluations are performed outside of the laboratory or in the absence of a treadmill. Without such data, comparisons of gait made across field testing sessions may be difficult to interpret as small changes in spatiotemporal, impact or attenuation may prove to be a function of speed. It is clear that more work needs to be done to address the relationships speed and gait characteristics and how they are affected by injury. At the very least, it is important to establish field testing protocols to insure consistent conditions across evaluation days.

An overarching goal of our recent series of papers (16, 17, 18) was to combine data from multiple wearable sensors to provide a more comprehensive approach to athlete monitoring. In the first two papers (17, 18) we showed how metrics derived by the manufacturer's analysis packages can be combined. In the final two papers (16, current study) we show the feasibility and applicability (i.e., proof of concept) of temporally merging raw data to examine gait. Wearable technology offers considerable benefits as measurements can be made in the field, resulting in high ecological validity of the data. Also, it is possible to simultaneously evaluate large numbers of athletes. However, there are a number of trade-offs. Not the least of which is the inability to tightly control the testing parameters across testing days and between individuals. In leu of controlling variables such as running speed, comprehensive monitoring can aid with interpretation of the data. Thus, trunk-mounted, GPS-embedded IMUs coupled with bilateral, ankle-worn IMUs can provide the necessary data needed to collect and evaluate data collected during field testing.

Practical Applications

This paper shows that foot-strike and toe-off events can be detected using ankle worn IMUs. When temporally synchronized with trunk mounted devices, spatiotemporal and impact attenuation variable can be generated. Application of these methods extend to use of wearable technology for examining gait characteristics in a large group of athletes, exercising outside of the laboratory. It is possible, that the data generated by these approaches can provide insight into potential changes in gait and gait asymmetries that occur due to conditions such a injury, rehabilitation and fatigue.

Limitations

- This study is limited by the small sample size (three health and three injured subjects). Thus, conclusions regarding the effects of ACL injury and reconstruction surgery on gait kinematics are tenuous.

- Straight-line running was used to assess gait kinematics. Thus, results may not be applicable to other types of running (e.g., curved, change of direction, etc.).

- Two different types of sensors were used, the STATSports APEX and IMeasureU BT-IMU. It is not known if the approaches used here are applicable to other types of sensors.

Twitter: Jay H. Williams (@sciscronline)

References

1. Aminian K, Najafi B, Büla C, Leyvraz P-F, Robert Ph. Spatio-temporal parameters of gait measured by and ambulatory system using miniature gyroscopes. J Biomech. 2002; 35: 689-699.

2. Button K, van Deursen R, Price P. Measurement of functional recovery in individuals with acute anterior cruciate ligament rupture. Br J Sports Med. 2005; 39: 866-871.

3. Derrick TR, Dereu D, McClean SP. Impact and kinematic adjustments during an exhaustive run. Med Sci Sports Exerc. 2002; 34: 998-1002.

4. Dufek JS, Mercer JA, Griffen JR. The effects of speed and surface compliance on shock attenuation characteristics for male and female runners. J Appl Biomech. 2009; 25: 219-228.

5. Hadizadeh M, Amiri S, Mohafez H. Roohi SA. Gait analysis of national athletes after anterior cruciate ligament reconstruction following three stages of rehabilitation program: Symmetrical perspective. Gait Posture. 2016; 48: 152-158.

6. Hunnicutt JL, McLeod MM, Slone HS, Gregory CM. Quadriceps Neuromuscular and physical function after anterior cruciate ligament reconstruction. J Athl Train. 2020; 55: 238-245.

7. Lee JK, Park EJ. Quasi real-time gait event detection using shank-attached gyroscopes. Med Biol Eng Comput. 2011; 49: 707-712.

8. Lewek M, Rudolph K, Axe M, Snyder-Mackler L. The effect of insufficient quadriceps strength on gait after anterior cruciate ligament reconstruction. Clin Biomech. 2002; 17: 56-63.

9. McGrath D, Greene BR, O'Donovan KJ, Caulfield B. Gyroscope-based assessment of temporal gait parameters during treadmill walking and running. Sports Eng. 2012; 15:

207-213.

10. Mercer JA, Bates BT, Dufek JS, Hreljac A. Characteristics of shock attenuation during fatigued running. J Sports Sci. 2003; 21: 911-919.

11. Mercer JA, Vance J, Hreljac A, Hamill J. Relationship between shock attenuation and stride length during running at different velocities. Eur J Appl Physiol. 2002; 87: 403-408.

12. Minning SJ, Myer GD, MAngine RE, Eifert-Mangine M, Colosimo AJ. Serial assessments to determine normalization of gait following anterior cruciate ligament reconstruction. Scan J Med Sci Sports. 2009; 19: 569-575.

13. Morgan KD. Using Time-Frequency Analysis to Characterize Altered Knee Dynamics in Post ACL Reconstruction Individuals. In2019 41st Annual International Conference of the IEEE Engineering in Medicine and Biology Society (EMBC) 2019 Jul 23 (pp. 2132-2135). IEEE.

14. Reenalda J, Maartens E, Buurke JH, Gruber AH. Kinematics and shock attenuation during a prolonged run on the athletic track as measured with inertial magnetic measurement units. Gait Posture. 2019; 68: 155-160.

15. Shorten MR, Winslow DS. Spectral analysis of impact shock during running. Int J Sport Biomech. 2002; 288-304.

16. Williams JH, Rizzuto SF, Dillard BA, Whitaker EJ. Complementary use of wearable technology 3: Temporal alignment and similarity measures of accelerometer signals from two IMU devices. Sport Perf Sci Rep. 2022; in review.

17. Williams JH, Rizzuto SF, Whitaker EJ, Dillard BA. Complementary use of wearable technology 2: A case study in gait symmetry. Sport Perf Sci Rep. 2021; Sep 138 v1.

18. Williams JH, Rizzuto SF, Whitaker EJ, Dillard BA. Complementary use of wearable technology 1: A data comparison of two platforms. Sport Perf Sci Rep. 2021; July 137 v1.